Original scientific papers UDK 697.329:519.677
doi: 10.7251/COMEN1501020P

LIQUID LEAD-BISMUTH EUTECTIC AS A COOLANT IN GENERATION IV NUCLEAR REACTORS AND IN HIGH TEMPERATURE SOLAR CONCENTRATOR APPLICATIONS: CHARACTERISTICS, CHALLENGES, ISSUES

Miroslav P. Popović[*], *Alan M. Bolind, Cristian Cionea, Peter Hosemann*
University of California, Berkeley, 2621 Hearst Ave, Berkeley, CA 94720, USA

Abstract: Heavy liquid metals have found a wide range of application in energy conversion systems, due to their beneficial thermal properties, especially their low melting points and their capability of operating at higher temperatures without boiling. In addition, the neutronic properties of various liquid metals make them attractive for fusion as well as in Generation IV nuclear reactors. Lately, concentrated solar power (CSP) systems have developed an interest in this technology, calling for temperatures up to 800 °C. The main challenge in realizing engineering scale units is to find proper structural materials that can withstand the corrosion and provide mechanical strength at operation conditions. Lead-Bismuth Eutectic (LBE) is one of the main candidate coolants for liquid metal cooled reactors and solar thermal power applications due to its physical properties such as good thermal conduction, low thermal expansion and melting point, non-violent reactivity to water and low neutron absorption. However, the key limiting factor for LBE usage is the fact of its high corrosiveness to steels and other structural materials. In this work, the results of our systematic materials study in liquid LBE and its alternatives are presented. Various potential structural materials were exposed to LBE, Rose's metal (Pb-Bi-Sn) and Pb-Bi-Zn eutectic, in static corrosion tests. Post corrosion characterization was conducted by microstructural analysis (SEM/EDS, X-ray diffraction, Raman spectroscopy) and preferential corrosion mechanisms were evaluated.

Keywords: liquid metals, lead-bismuth eutectic, solar energy, nuclear systems, corrosion, steel.

1. INTRODUCTION

Liquid lead-bismuth eutectic (LBE) became a focus of thorough research several decades ago, particularly in Soviet Union and Germany, as a potential heat-transfer fluid in nuclear applications, mainly nuclear power plants and submarines, due to its preferred thermophysical properties (heat capacity, thermal conductivity, thermal expansion coefficient, etc.), and nuclear properties. This research has produced a large database of LBE properties, which is helpful as a starting point for any further research [1]. Although these research efforts experienced a standstill through the 1990s, after the collapse of the Soviet Union and the change in global policy, interest in liquid-metal coolants was revived when the Generation IV Fast Reactor program was proposed.

The increase in global electrical energy demand in recent decades [2], coupled with a parallel global temperature increase expected for the same period, has increased the need for carbon-free energy sources, as well. Concentrated solar power (CSP) can contribute to the electricity production portfolio as a green house gas free alternative energy source. It has the potential to achieve low costs in the long term due to their ability to reach high temperature and utilize more efficient thermo-dynamic cycles [3, 4]. Also, the direct hydrogen production from water in CSPs, which is possible if the heat-transport-fluid temperature reaches 900 °C makes them economically competitive. Moreover, combining CSP with either thermal or hydrogen storage allows an energy production for 24 hours a day, since the stored energy (heat or hydrogen) can be used during night to keep the electric supply stable. However, CSP performance over 800 °C is a challenge, and new, possible heat-transfer fluids need to be considered.

[*] Corresponding author: popovic@berkeley.edu

Oil-based fluids cannot be used in such high-temperature applications because of their disintegration at temperatures over 600 °C [5]. On the other hand, gases have low density and therefore less efficient heat transport, while molten salts are known to have high melting points [6]. These facts leave only liquid metals as potential candidates. Among them, there are two categories of metals used: light (very reactive) metals - among which sodium is the main one, and heavy liquid metals – among which lead and lead-based alloys are best known and used. While being hazardous when in contact with water, sodium seems to be an unlikely candidate for high-temperature applications due to its boiling point being slightly above 800 °C at 1 atm pressure. Such a relatively low boiling point can lead to a significantly more dangerous situation if sodium vapor is released at high temperatures, since it will burn upon contact with moisture from the air. For these reasons, only liquid heavy metals remain as reasonable candidates for high-temperature applications.

The main properties liquid metals must possess in order to be candidates for use in CSP systems and in nuclear reactors are low melting point, high heat capacity, good thermal conductivity, relatively low viscosity, and low corrosiveness and low costs if possible. Historically, large facilities have been built and successfully operated – which leads to a significant amount of research experience in working with various liquid metals and alloys, mostly with lead and lead-bismuth eutectic, LBE (55.5 w. t.% Bi, 45.5 w. t.% Pb) [5].

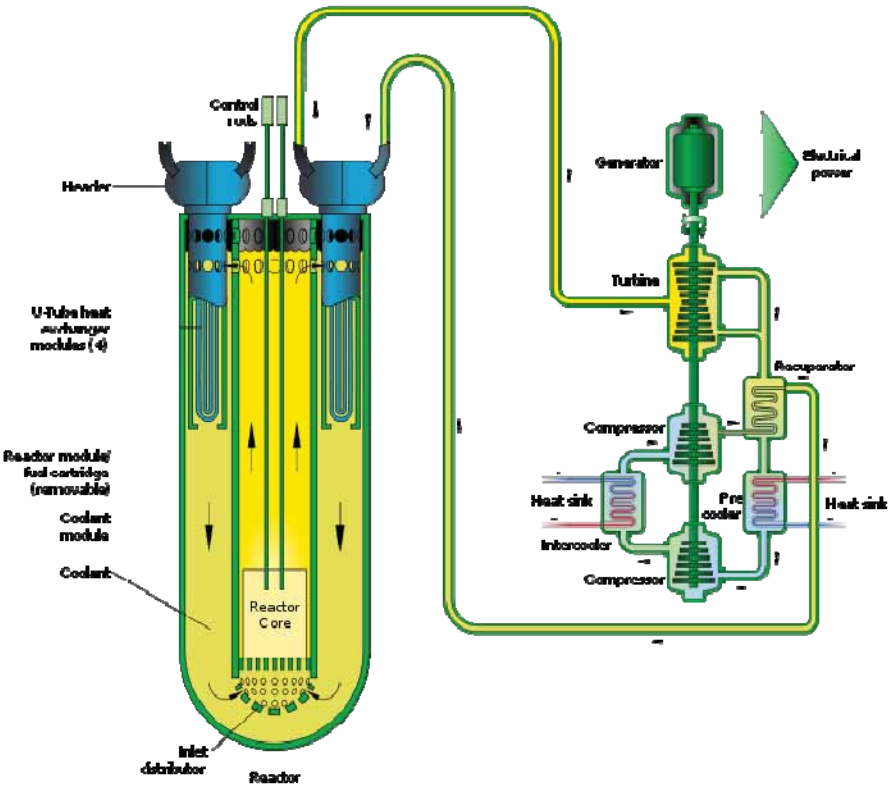

Figure 1. A scheme of a Liquid-Metal-cooled Fast Reactor (LMFR) [7]

This leads to a large amount of data that has been obtained from nuclear application, where LBE has been used as a coolant in liquid-metal-cooled fast reactors (or *liquid metal fast reactors*, LMFR, see Figure 1), first adapted for nuclear submarine use, but later also for power generation [5]. A special benefit of this alloy is the large temperature difference (ΔT) between the high boiling point (1670 °C) and the rather low melting point (125 °C) [7]. The other benefits are non-reactivity with water and a low vapor pressure as well.

A general issue about the use of LBE is its corrosiveness, and a main obstacle to its deployment as a heat transport fluid is finding structural materials that can withstand its harsh corrosion environments at high temperatures, including the possibility of liquid-metal-assisted embrittlement [15]. The combination of corrosion, long-term operation and

structural integrity over a wide range of operating conditions make the structural materials choice rather challenging for temperatures above 600 ºC. Hence, the main goals of research in this area are (1) to design a liquid metal composition with suitable corrosion and thermophysical properties at temperatures of 600−800 ºC, (2) to find the best candidates for structural/piping material, and (3) to determine a proper liquid metal chemistry. The criteria for liquid metal alloys selection are wide liquid-phase range, good thermal properties, low corrosivity and toxicity, commercial accessibility, and low reactivity with air and water. Only several elements from the periodic table, when combined together in suitable alloys, can meet all these criteria: lead, bismuth, tin, zinc and antimony.

2. OXYGEN CONCENTRATION CONTROL IN CORROSION TEST SYSTEMS

Many structural materials (steels) from which the system components are manufactured (and with which the liquid metal comes into contact) – like iron (Fe), chromium (Cr) and nickel (Ni) – have a high solubility in heavy liquid metal alloys at temperatures greater than 400 °C, and this solubility increases with further temperature increase. This solubility can lead to extensive dissolution of these structural-material elements if there is no mechanism to prevent it, but the dissolution can be reduced by the presence of a passive oxide film on the structural materials surface. Diffusion of the material's atoms through the oxide layers then becomes the rate-limiting step for the dissolution corrosion [8,9]. Such passive oxide films can be grown through the use of an active oxygen-control system, which adds or removes oxygen from the heavy liquid alloys, as needed [8]. Active oxygen control is possible because lead and bismuth are less chemically active than are the main constituents of steel and other common structural materials; the formation of their oxides produces higher Gibbs free energy changes (ΔG) than does the formation of the oxides of the structural materials. The ΔG of chemical compound formation is in direct proportionality with the electric potential of its formation (measured as the electromotive force), as given by relation:

$$\Delta G = -nFE ,$$

E is electromotive force (EMF). This equation means that ΔG can be expressed by the electric potential, or EMF, and precisely measured and controlled in that way. This effect is well illustrated by the Ellingham diagram (Figure 2) where the free energy lines of Fe_3O_4, Cr_2O_3 and Al_2O_3 lay below the free energy lines of Pb- and Bi-oxides, thus allowing the formation of iron, chromium and aluminum oxides on the surface of steel.

However, high oxygen content in liquid Pb and Bi alloys can generate Pb and Bi oxides that precipitate in colder sections of coolant systems (causing clogs in pipes and tubes), and it can also lead to fast oxidation rates of the steel surface. Therefore, a balance between high and low oxygen content is essential for developing a reasonably low corrosion rate based on protective oxide films.

The optimal oxygen content in LBE as a function of temperature is shown in Figure 3, where the upper edge of the square defines the oxygen concentration needed to prevent the formation of lead oxides, while the lower edge defines a concentration that allows the formation of mixed iron-oxide in the given temperature range. The oxidation in liquid metal is a dissolution-oxidation process rather than a straight oxidation (illustrated in Figure 3, where excessively oxidized Fe-Cr-Al steel at high oxygen content and dissolution at low oxygen content can be seen in the Scanning Electron Microscopy (SEM) images of a solid sample). [5] The optimal oxygen content for LBE systems operating between 550 °C and 800 °C is known to be in the range between 10^{-4} and 10^{-6} wt.% of monoatomic oxygen (considering Fe-oxides formation only) [11,12]. A similar range is supposed to be for the other Pb/Bi-based heavy alloys tested here. While oxygen concentration is in the operational range (defined for a particular liquid metal, solid material and specific temperature), the protective layer is being formed. In fact, Al_2O_3 and Fe-Cr-spinels are the specific oxides that form the basis of protective layers (protective oxides), which means that the minimum required oxygen content moves towards lower values (down to 10^{-7}−10^{-8} w. t.%), therefore making it easier to control.

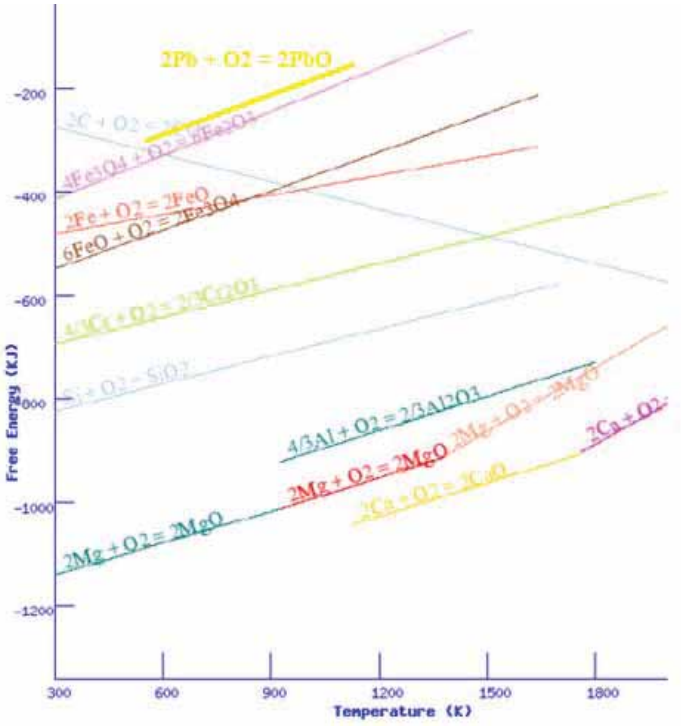

Figure 2. Ellingham diagram of specific oxide formation for carbon (C) and several metals, calculated by the Ellingham Diagram Web Tool (ref. [10]). Lead (Pb) and main steel-constituting elements (Fe, Cr, Al) shown as well.

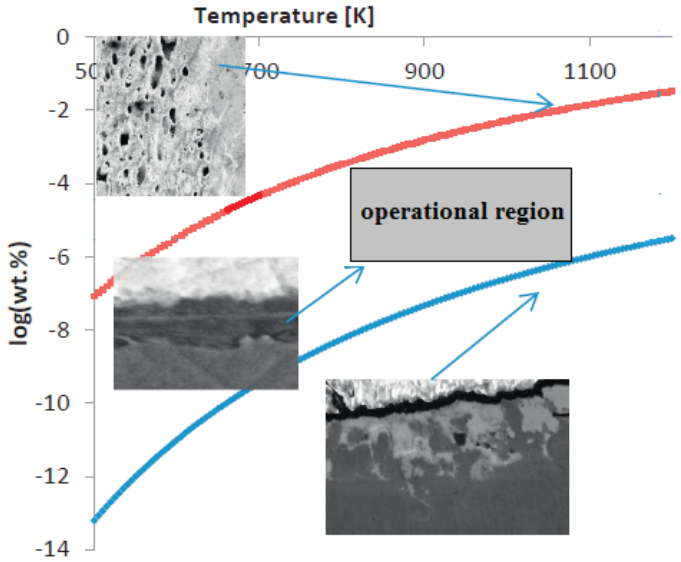

Figure 3. Oxygen concentration range in LBE for the temperatures in the range of 500 – 1200 K. The operation region presents the optimum oxygen concentrations in the temperature range of 823 – 1073 K (550°- 800°C) used in this research (right and left edge of the gray square), assuming that PbO formation should be avoided and Fe_3O_4 allowed. The oxygen content determining the upper limit is the solubility of O_2 in LBE; the lower means the concentration of O_2 needed to form magnetite, Fe_3O_4 (magnetite here serves only the purpose to illustrate the narrowest 'window'). Bottom right image: a penetration of LBE into material due to a too low O_2 concentration (not enough for protective oxide layer formation). Top left image: a porous structure in steel material caused by the fast oxidation rate in material due to a high O_2 concentration in liquid (illustrations from the experiments done at UC Berkeley [5])

A precise oxygen control of the liquid metal is crucial to maintaining and growing self-healing protective oxide layers on steel. For measuring and controlling the oxygen content of liquid metals at temperatures up to 800 °C, commercially available oxygen sensors can be used. In liquid metals, the oxygen sensor allows the transport of O^{2-} ions through the sensor's tip (yttria stabilized zirconia), thereby allowing the measurement of the electrochemical potential (i. e. electromotive force, EMF) between the oxygen in the reference (Pt/air) of the sensor, and the oxygen in the liquid metal. The

oxygen concentration of the liquid metal can be calculated based on the modified Nernst equation (for a general oxidation reaction, $xM + (y/2)O_2 \rightarrow M_xO_y$):

$$EMF_{M_xO_y} = -\frac{1}{4F}\Delta_f G^0_{\frac{2}{y}M_xO_y} + \frac{RT}{2F}\left\{\frac{x}{y}\ln(a_M) - \frac{1}{y}\ln\left(a_{M_xO_y}\right) + \frac{1}{2}\ln\left(a_{O_2\ in\ air}\right)\right\} \quad \text{Eq. (1)}$$

where the first term on the right hand side is the standard Gibbs free energy of metal oxide formation at the standard T and P, the $(RTx/2Fy)\cdot\ln(a_M)$ represents chemical activity of a non-oxidized metal in the reaction, while the next term, $\left(\frac{2}{y}\right)\frac{RT}{4F}ln\left(a_{M_xO_y}\right)$, means the chemical activity of metal-oxide in the reaction system. R is the universal gas constant; T is absolute temperature; F is the Faraday constant; $\Delta_f G^0_{\frac{2}{y}M_xO_y}$ is the Gibbs free energy of formation of $2/y$ moles of M_xO_y oxide at temperature T and when the activities of the reactants and products are equal to unity; a_M is the activity of the oxidizing metal (equal to 1 if the metal is solid or if the liquid metal is purely this oxidizing metal; less than 1 if the metal is only a part of the liquid alloy); $\alpha_{M_xO_y}$ is the activity of the oxide (equal to 1 if the oxide is forming a scale on the solid metal or is precipitating out of the liquid metal; less than 1 if the oxide is an oxide of one of the liquid-metal constituents and is not precipitating out of solution); and $\alpha_{O_2 in\ air}$ is the activity of oxygen in the air reference of oxygen sensor, which is exactly *0.2095* (or 20.95%, i. e. the percentage of O_2 in the air). This means that the last term in the previous equation can be given as

$$\frac{RT}{4F}ln\left(a_{O_2,atr}\right) \approx \frac{RT}{4F}\ln(0.2095) \quad \text{Eq. (2)}$$

However, the activity of metal oxide is

$$a_{M_xO_y} = \frac{c_{M_xO_y}}{c^{saturation}_{M_xO_y}} \quad \text{Eq. (3)}$$

meaning that only the ratio on the right hand side can be found. In order to find a concentration (numerator in the equation), the denominator of equation must be found first – by an independent measurement (such as mass spectrometry or coulometric titration). In this way, the EMF measured in oxygen sensor is a function of temperature (T) and of the activity of metal oxide (a_{MxOy}), i.e.

$$EMF_{M_xO_y} = f(a_{M_xO_y}, T) \quad \text{Eq. (4)}$$

If the measured EMF is less than the EMF for oxidation of the metal, the metal will oxidize. (In the Ellingham diagram, oxidation occurs if the Gibbs free energy that corresponds to the system's oxygen activity is less negative than the Gibbs free energy of the oxide formation; see Figure 4). It is not necessary to know the oxygen concentration in the liquid metal in order to know and control the oxygen activity at one specific temperature: the measurement of the EMF alone is sufficient to control the oxidation power of a liquid alloy at that temperature. By setting an EMF value below the line of formation of protective steel oxides, it can be proved thermodynamically that those oxides are able to form (although the oxide layer formation also depends on kinetics of the process).

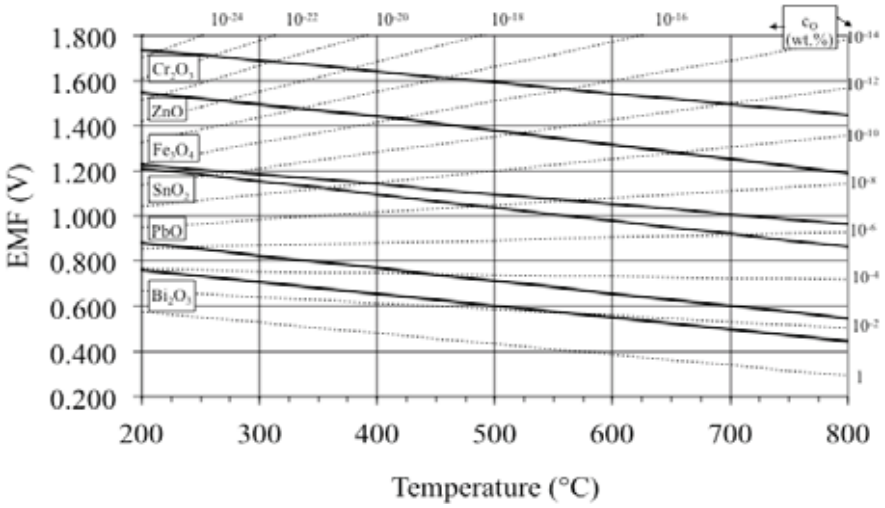

Figure 4. A relationship between the EMF of various metal oxides' formation (measured by the air-referenced oxygen sensor), the temperature (solid lines), and the monatomic oxygen concentration (w. t%, dotted lines) in liquid LBE. The actual concentration of metal oxide assumed to be in saturation (a = 1) [14]

3. MATERIALS SELECTION

Having in mind the elements from the periodic table that can meet the selection criteria for possible use in high-temperature liquid metal alloys, and knowing the principles of oxygen concentration control (previous section), a down-selection (a design) of liquid-alloy candidates can be made; this selection was the main part of the work described in this paper. The priority in this study was both the evaluation of candidates (in both qualitative and quantitative ways) and the understanding of the corrosive effects of the constitutive elements, at liquid-metal temperatures higher than in any previous research in this area.

Initial screening of liquid-metal alloys was made by calculating their thermal properties (such as liquidus temperatures) with the CALPHAD thermodynamic approach, and by performing thermal analysis on small samples of alloys (for example, by differential scanning calorimetry). LBE remains the main candidate for testing at high temperatures, for two reasons. First, the long history of scientific investigation of this alloy as a heat-transfer fluid in nuclear applications (though in the temperature range $\leq 550^0$C) has produced a lot of data on its properties, which is available in the literature. Second, Pb and Bi exhibit a lower tendency to form intermetallic phases with the common constituents of structural metal alloys (Fe, Cr), and the structural metal alloys exhibit relatively lower solubility in LBE than in other possible liquid metals. Besides LBE, two other lead-bismuth-based alloys have been tested in our work thus far: Rose's metal (50 wt% Bi, 25 w. t.% Pb, 25 w. t.% Sn), and Pb-Bi-Zn alloy (near eutectic; 61.5 w. t.% Pb, 37.5 w. t.% Bi, 1 w. t.% Zn). These alloys were chosen as variations of the LBE that enable more straightforward evaluation of the corrosive effects of Sn and Zn (their tendency to form intermetallics), while still maintaining sufficiently low liquidus temperatures.

Table 1. Eutectics chosen for examination in static corrosion tests.

	Pb w. t.%	Bi w. t.%	Sn w. t.%	Zn w. t.%	$T_{melt.}$ °C	Type of protective layer
LBE	44.5	55.5			125	Oxide
Pb-Bi-Sn	25	50	25		95	Oxide
Pb-Bi-Zn	61.5	37.5		1	~ 120	Intermetallics

In order to find structural (pipe) materials appropriate for use in high-temperature liquid metal environment, a thorough discrimination/selection of candidates needed to be done. High-nickel-containing materials, such as SS-316L and Inconel-693, showed an excessive dissolution after staying for 500 or more hours in LBE at 700°C, due to nickel being highly soluble in liquid LBE, and so were rejected from further study. Aluminum-based alloys were abandoned because of their too low melting temperature (~ 660 °C), while titanium and refractory metals have been excluded due to their excessive oxidation in the air that surrounds the outsides of the pipes that contain the liquid metal. Hence, of all possible structural materials, only ferritic steels (having no nickel) remained as candidates. Kanthal steels have proved thus far to be the materials of choice (a list of the tested Kanthal steels is given in Table 2), because of their availability, cheapness, absence of Ni, and high content of Cr and Al – crucial elements for the formation of protective oxide layers on the surfaces of the structural material.

Table 2. Composition of the Kanthal steel candidates used as structural materials in the static corrosion testing (data taken from Sandvik, the manufacturer)

	C (w. t.%)	Si (w. t.%)	Mn (w. t.%)	Mo (w. t.%)	Cr (w. t.%)	Al (w. t.%)
ALK	< 0.08	< 0.7	< 0.7		12.0–14.0	4.0
APM	< 0.08	< 0.7	< 0.4		20.5–23.5	5.8
APMT	< 0.08	< 0.7	< 0.4	3.0	20.5–23.5	5.0

4. STATIC CORROSION TESTS – SETUP AND PROCEDURES

A setup for oxygen-controlled static corrosion tests has been developed in order to perform selected materials examination. Each static corrosion test was conducted in an alumina crucible inside an autoclave, as illustrated schematically in Figure 5 [17]. The oxygen content of the cover gas inside the autoclave was maintained actively by switching the gas flow between diluted hydrogen (5% H_2, balance Ar) and diluted oxygen (3% O_2, balance Ar) through the autoclave, based on the electromotive-force (EMF) readings coming from the oxygen sensor that was immersed into the liquid metal. As explained above in Section 3, the EMF, or voltage, was produced by the oxygen sensor because of the difference in oxygen activities between the oxygen in the air in the sensor's reference (at 20.95%) and the oxygen in the liquid metal.

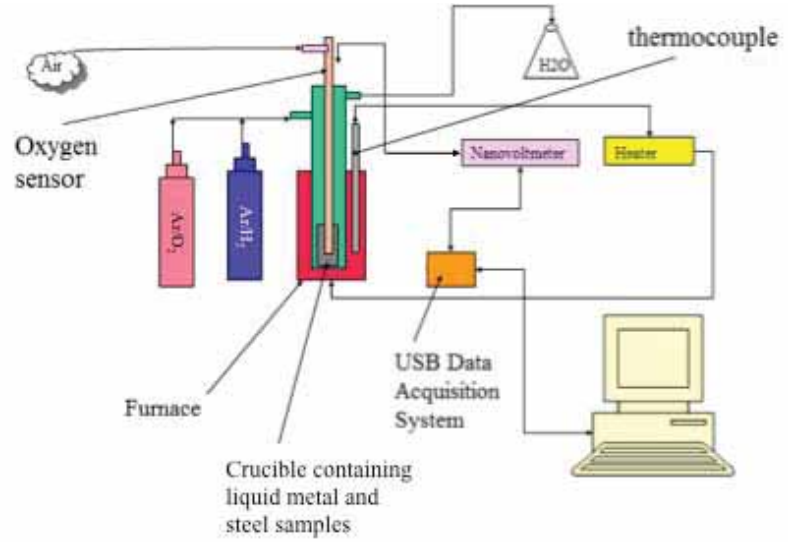

Figure 5. A schematic of a static corrosion test setup [17]

In order to establish a proper oxygen control in the system, the EMF must be precisely measured and maintained within the correct range. For this purpose, the output of each gas bottle is equipped with the gas control valve that has a feedback connection to the data acquisition software for EMF control. A correlation between EMF and oxygen content in the reaction system can be given by the following quick rule of thumb: the higher the oxygen concentration, the lower the EMF in the system. For instance, in LBE at 700 °C, according to the modified Ellingham diagram with the dashed lines of oxygen concentration (Figure 4), the point of EMF = 1.0 V corresponds to ~ 2 10^{-7} w. t.% oxygen. At this position, the EMF is close to the line of Fe_3O_4 formation, far below the Cr_2O_3 and Al_2O_3 lines, and far above the lines of PbO and Bi_2O_3 formation. This fact means that with this oxygen concentration at this temperature, Cr_2O_3, Al_2O_3 and Fe_3O_4 can be formed, but PbO and Bi_2O_3 cannot. If the EMF goes slightly upwards on this chart, the oxygen concentration goes down: so, for EMF = 1.1 V, the oxygen concentration is ~ 10^{-8} w. t.% and is above the Fe_3O_4 formation line, thereby preventing the mixed iron oxide formation.

Each one of the three Kanthal samples was polished and then cut into three long, thin strips of nearly the same size after polishing, and immersed into a molten alloy (at 600−800 °C) for a defined time period, up to 1000 h, and continuously under the flow of one or the other of the gases (Ar/H_2 or Ar/O_2), so that the desired EMF value could be kept constant. Each strip was dipped vertically partway into in the liquid metal and was held in place by passing it through a slot in a holder that sat on top of the crucible. To obtain the mid-term results, one strip of each one of the steels was pulled out from its slot and analyzed; these pullouts were done after three different lengths of time.

In the case of LBE, the analytical formula of correlation between EMF and oxygen concentration in liquid metal (ref. [11], p. 160) was used. For Rose's metal and Pb-Bi-Zn, there was no analytical equation for EMF as a function of temperature and oxygen concentration, since such an equation requires the use of an independent measurement, such as by coulometric titration, of the saturation oxygen concentration in Pb-Bi-Sn and Pb-Bi-Zn as a function of temperature. Therefore, EMF was determined and set (in each test) on a value that is

in-between the potentials of iron-oxide formation (the minimum one) and the formation of the oxide of the most reactive liquid-metal constituent, which was Zn in the case of Pb-Bi-Zn eutectic and Sn in the case of Rose's metal).

The candidate liquid metals were Pb-Bi (LBE), Pb-Bi-Sn (Rose) and Pb-Bi-Zn eutectic systems, at temperatures 600−800 °C (Table 1). As a characteristic, all of them have low melting points (< 150 °C) and have the potential of forming either oxide or intermetallics with Kanthal steels in the presence of oxygen. Three long-term static corrosion tests (Table 3) have been performed in LBE, two in Rose's metal, and three in Pb-Bi-Zn, using three Kanthal steels (ALK, APM, APMT) as the structural materials in all the tests. The tests cover temperatures in the range 600−800 °C, various time periods up to 1000 hours, and various oxygen concentrations in the system. Results from the static corrosion tests in LBE, Rose's metal and Pb-Bi-Zn eutectic were analyzed by scanning electron microscopy (SEM) and energy dispersive x-ray spectroscopy (EDS) in order to assess the structural material (bulk metal) loss in three Kanthal steel samples (ALK, APM, APMT) caused by the exposure to the liquid metals.

Table 3. A list of the long-term constant-temperature static corrosion tests performed. The concentration of oxygen in Pb-Bi-Sn (Rose's metal) and Pb-Bi-Zn was approximately assessed, since the exact dependence of the electromotive force on the oxygen content in the system, EMF = f(c_O, T), is yet unknown for these alloys.

Liquid Alloy	Temperature (°C)	Max. duration (hours)	EMF set point(V)	Oxygen concentration (wt%)	Number of pullouts
LBE	700	1000	0.918	10^{-6}	3
LBE	800	1000	0.926	10^{-6}	3
LBE	800	440	1.014	10^{-7}	2
Rose's Metal	700	500	No oxygen control	No oxygen control	1
Rose's Metal	700	920	0.918	At formation of SnO_2 (Conc. unknown)	3
Pb-Bi-Zn	600	1000	0.98	High ($\geq 10^{-6}$)	3
Pb-Bi-Zn	700	440	0.90	High ($\geq 10^{-6}$)	2
Pb-Bi-Zn	800	440	0.93	Low ($\sim 10^{-7}$)	2

5. RESULTS OF HIGH-TEMPERATURE STATIC CORROSION TESTS IN LBE AND ITS DERIVATIVES

5.1. LBE: corrosion behavior

Three successful long-term static corrosion tests in liquid LBE have been performed (Table 3). In the first two listed in the table (700 °C and 800 °C, 10^{-6} w. t.% oxygen ; pullouts of samples after 350 h, 700 h, and 1000 h), the ALK steel performed acceptably well. It tended to form a fairly adherent, inner, Al_2O_3 layer of 4 μm thickness and an outer, chromium-rich oxide layer of about the same thickness. An example of such aluminum and chromium oxide layers is shown in Figure 6. The oxide-scale thickness did not consistently grow larger over time, probably because the scale detached and reformed one or more times, as indicated by the presence of remnants of aluminum oxide in the LBE near the surface of the steel at longer immersion durations. The detachment of the oxide layer could have been caused by the thermal cycling and/or the handling of samples when the mid-term samples were obtained. If the dissolution is estimated as being ~12 μm, based on SEM micrographs of dissolution zones of this depth into the steel, then the total corrosion depth of oxide plus dissolution can be estimated at 16 μm after 1000 hours of immersion. This corrosion rate corresponds to less than 140 μm per year, which is fairly acceptable.

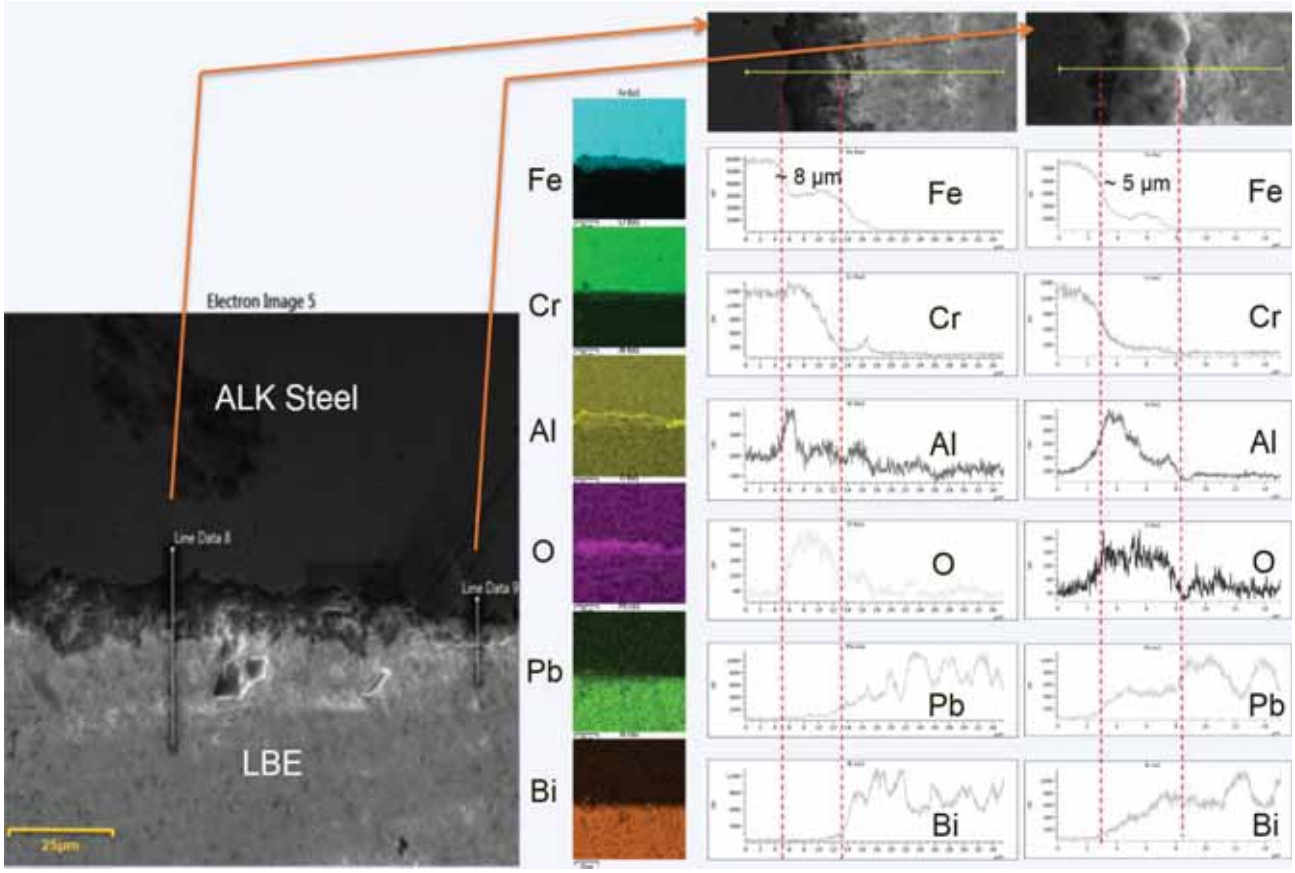

Figure 6. SEM and EDS analysis of a cross section of the interface between ALK and LBE, after exposure for 633 hours at 700 °C with 10^{-6} w. t.% oxygen (EMF = 0.917 V)

The APM and APMT steels did not fare quite as well as the ALK did, in constant-temperature LBE; their oxides were less adherent; and as a consequence, there was significant more dissolution in both steels at the longer immersion durations. Figure 7a shows a worst-case example of the dissolution of APMT. APM and APMT steels have only a limited capability of re-forming the protective oxide (mainly Al_2O_3) at this condition. Where the oxide layer failed; a residual oxide layer was frequently found (on the SEM scan) „floating" in the LBE near the original steel surface after the substrate steel had been completely dissolved away. At other places where the oxide layer adhered, little to no dissolution occurred. Frequently, the oxide layer was even thicker in APM and APMT than in ALK, meaning a smaller material loss to oxidation in the latter (Figure 8). Thus, the corrosion performance of these steels appears to depend on various surface conditions of the steels or on other factors.

The third LBE test in Table 3 (800 ^{o}C in the 10^{-7} w. t.% oxygen, at 440 h) indicates that 10^{-7} w. t.% oxygen at 800 ^{o}C is not enough for controlled oxide layer formation in any of the three Kanthal steels, so that there were only destruction of the material and a thickness loss of 60−140 µm, even after only 220 hours (Figure 9 and Table 10).

Some of the detachment of the oxide layers in LBE experiments might have been caused by the handling of the samples during extraction from the liquid metal and preparation for microanalysis. Another cause might have been the difference in the thermal expansion coefficients of the oxide layer and of the substrate steel; detachment would then have occurred during the cooling down of the sample prior to extraction.

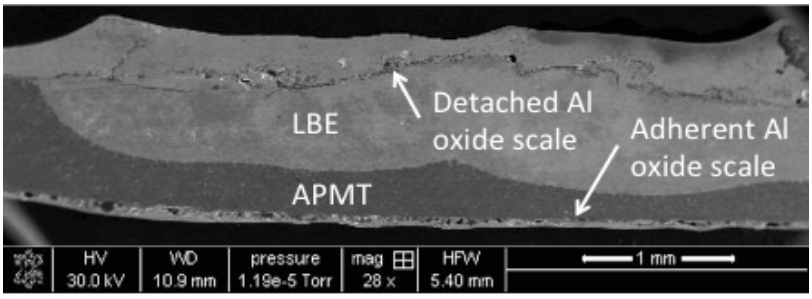

a)

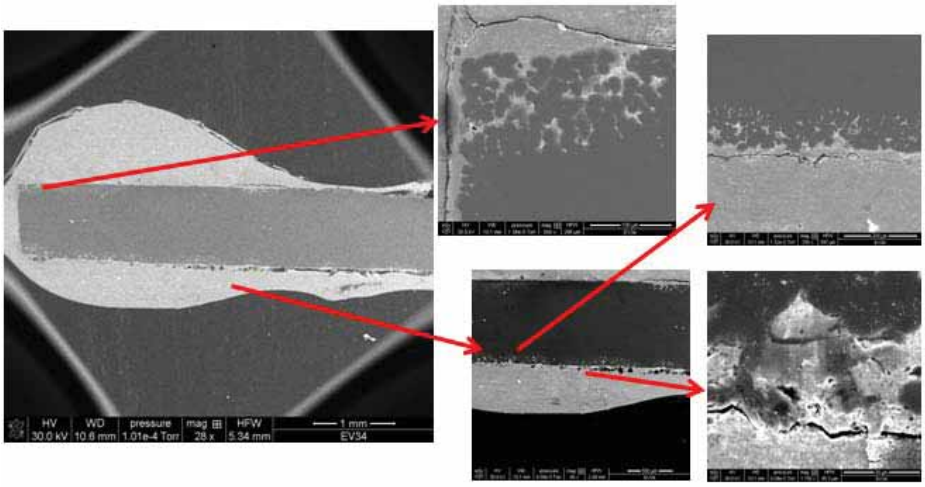

b)

Figure 7. a) Worst-case example of the dissolution of APMT after 1000 hours in LBE at 800 °C/10^{-6} w. t.% oxygen (EMF = 0.926 V). b) SEM images of a cross section of APM Kanthal steel after 1000 hours in LBE at 700 °C/10^{-6} w. t.% oxygen (EMF = 0.918 V). Penetration of liquid into APM bulk.

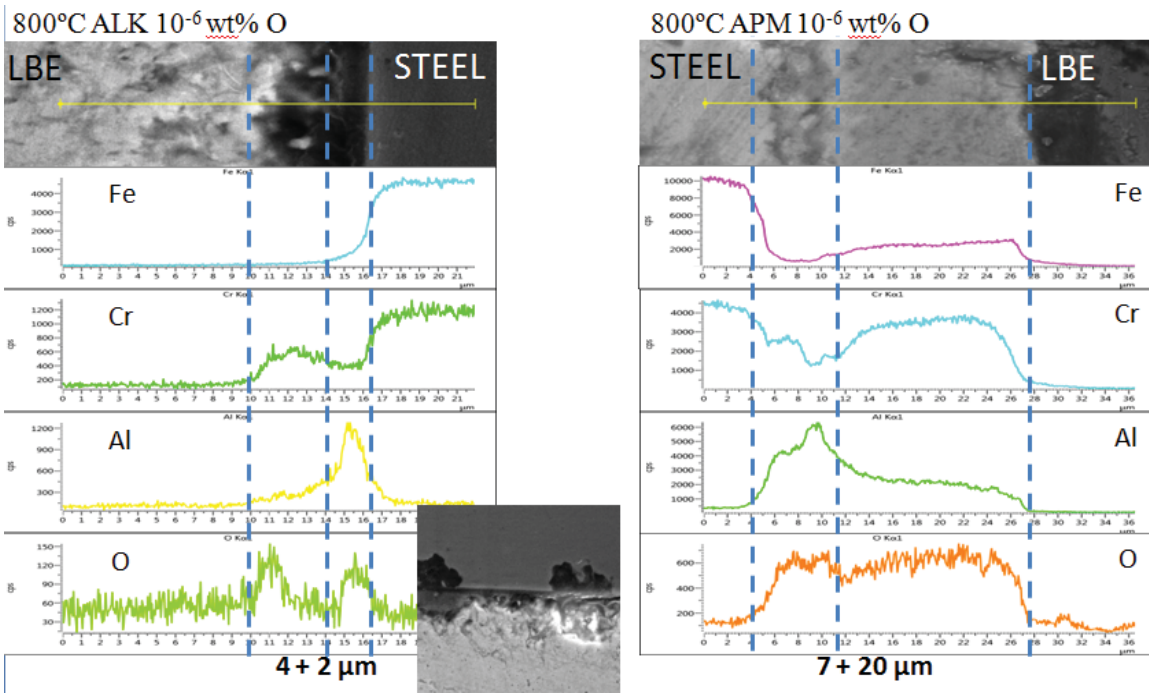

Figure 8. EDS results for ALK (left) and APM (right) at 800 °C after 1000 hours of exposure. A thinner protective oxide layer (less loss of material to oxidation) was detected in ALK than was detected in APM

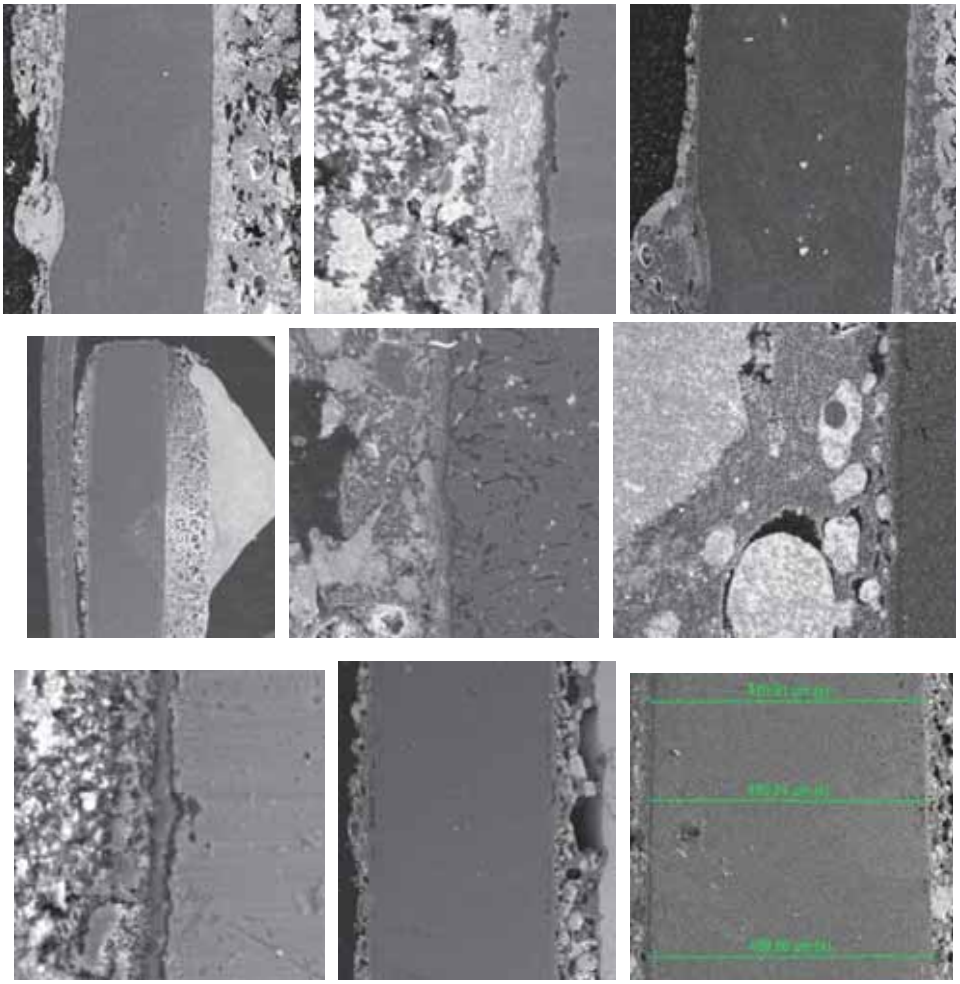

a) ALK

b) APM

c) APMT

Figure 9. Not enough protective oxide layer on the surface of Kanthal samples after 220 hours of treatment in LBE at 800 °C in low oxygen concentration (10^{-7} w. t. % oxygen)

5.2. Rose's metal: corrosion behavior

Kanthal steels dissolved more in Rose's metal than they did in LBE. This finding is not surprising given that Sn more readily forms intermetallic phases with Fe and Cr than Pb or Bi forms with these elements, according to phase diagrams. Therefore, Sn in liquid Rose's metal can be expected to accelerate the dissolution of these steel constituents into the liquid.

As in the LBE tests, the ALK steel performed the best in the oxygen-controlled Rose's metal tests and did not experience massive dissolution even after 920 hours of immersion (Figure 10). This performance can be attributed to evidence that even though the aluminum oxide layers sometimes detached from the ALK surface, a new oxide layer formed on the freshly exposed surface. If it is estimated that at most three 4 μm thick aluminum oxide layers spalled off during 920 hours, accompanied by 4 μm of dissolution at most, then the corrosion rate of ALK in Rose's metal is again less than 150 μm per year at 800 °C, as it is in LBE.

The better protective properties of ALK can be ascribed to the differences in structural elements content: a lower content of Cr (12−14 w. t.%) and Al (4%) in ALK than in APM and APMT (20−23 w. t.% of Cr, and 5−6% of Al), along with a higher content of manganese (~ 0.7% in ALK, < 0.4% in APM/APMT). This finding seems to indicate that it is possible to have too much Al in the steel for corrosion protection; the optimum amount is somewhat less than the maximum amount allowable from the metallurgical perspective. The thicknesses of the oxide layers formed in Rose's metal were almost the same, or very similar, to those formed in LBE in the equivalent (corresponding) pullouts. However, the oxide layer detachment seemed to be more frequently present here in this alloy, and much more penetration of Rose's metal (i. e. dissolution of structural material) occurred in APM and APMT than in ALK (Figure 11).

Because of tin's greater affinity for oxide formation relative to the oxides of lead and bismuth (thus narrowing the window for oxygen control), and because of the more frequent oxide layer detachment from the steels in Rose's metal, resulting in abrupt and massive dissolution of the material, Rose's metal has been abandoned in further research and dropped from the list of liquid alloy candidates.

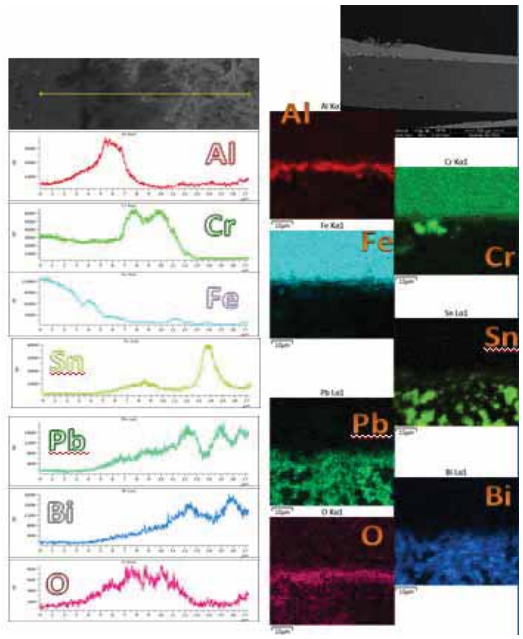

Figure 10. SEM and EDS scans of cross section of the interface between ALK Kanthal steel and Rose's metal after 1060 h of exposure in Rose's metal at 700 °C, at the potential near the oxygen saturation point (EMF = 0.918 V). There is about 3 μm of Al_2O_3 inner layer (towards steel), and about 5 μm of Cr_2O_3 outer layer (towards Rose's metal).

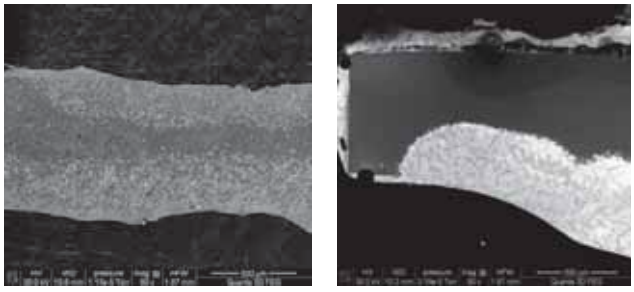

Figure 11. SEM scan of the cross sections of solid-liquid interface in APM and APMT Kanthal steels, after 1060 h in Rose's metal at 700 °C. Massive dissolution is visible (liquid metal penetration) in both APM (left) and APMT (right)

5.3. Pb-Bi-Zn eutectic: corrosion behavior

Three tests have been performed in Pb-Bi-Zn eutectics (Table 3). Results of SEM/EDS analysis show that there was a strong formation of an intermetallic layer on the surfaces of all three Kanthal steels. The layer was thick and fully attached to the bulk, having almost all elements from liquid and bulk therein. This result implies a large and uniform loss of the bulk metal material, i.e. a noticeable sample thickness loss (although there was a lack of intermetallic layer detachment, potentially considered as an advantage). In addition, the depletion of bulk structural elements (Fe, Cr, Al), by penetration of liquid Pb-Bi-Zn into solid and the increase of intermetallic layer thickness, caused a mechanical weakening and embrittlement of the samples, subsequently leading to their cracking and breaking while being handled.

Since it was difficult to characterize the material loss (as a total change in sample thickness) in the absence of oxide layers to indicate the original surface, the thickness change was characterized as a total thickness of the intermetallics zone. The intermetallic zone was compact and well-attached to the bulk steel and contained various elements from both bulk and liquid, but very thick and heterogeneous (Figure 12), with erratic and unpredictable changes in layer thickness in time (Figure 13) indicating a significant structural material loss in Kanthal samples. In fact, a bit unexpected decrease of layer thickness in time (in samples exposed for 1000 h) indicates that even the previously formed intermetallic layer (and not only the bulk metal) suffers a dissolution in a protracted contact with liquid, so that the protective function of layer is compromised (at least at 600 °C).

Another way to characterize the loss of material is by measuring the depth of penetration of the liquid into the solid (for the areas where there is no protective layer formation, but liquid penetration/solid dissolution only). This method shows again better results in the case of LBE (less material loss, lower penetration) than in the case of Pb-Bi-Zn (Figure 14).

In general, Pb-Bi-Zn alloy cause a thick, extensive, and non-protective intermetallic layer on the surfaces of Kanthal steels, particularly at higher temperatures. These intermetallics consume a large amount of bulk material, hence causing a large material loss (see Table 4) and a subsequent decline of the mechanical integrity of a structure due to the thickness loss.

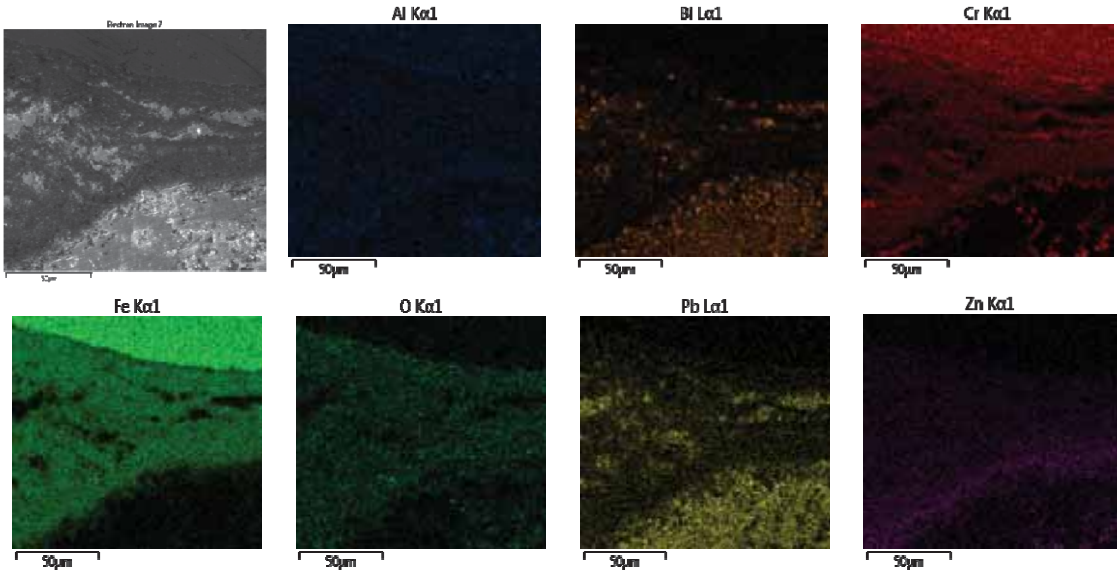

Figure 12. SEM (a) and EDS maps of the sample APMT exposed to Pb-Bi-Zn (add concentrations) after 440h exposure at 700 °C, at EMF = 0.90 V.

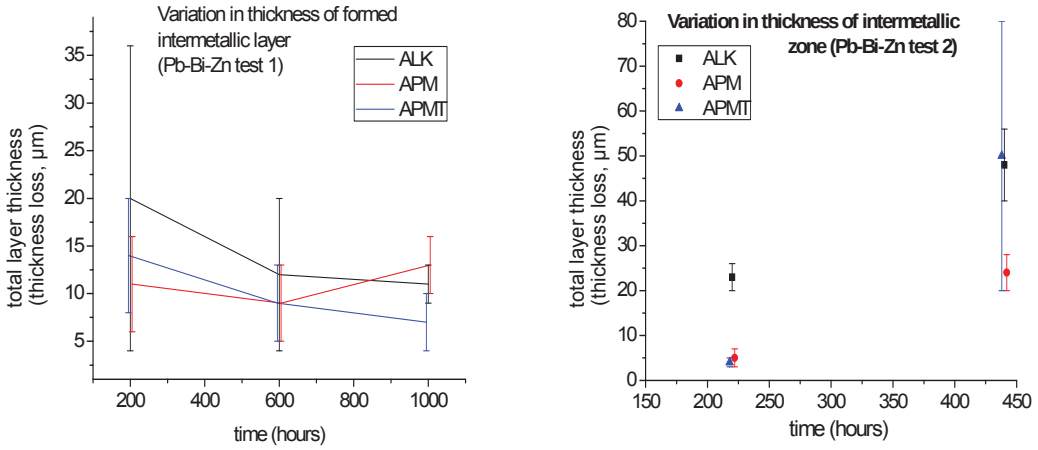

Figure 13. Bulk material loss – intermetallics zone thickness, Kanthal steels in Pb-Bi-Zn eutectic at 600 °C (left) and 700 °C (right)

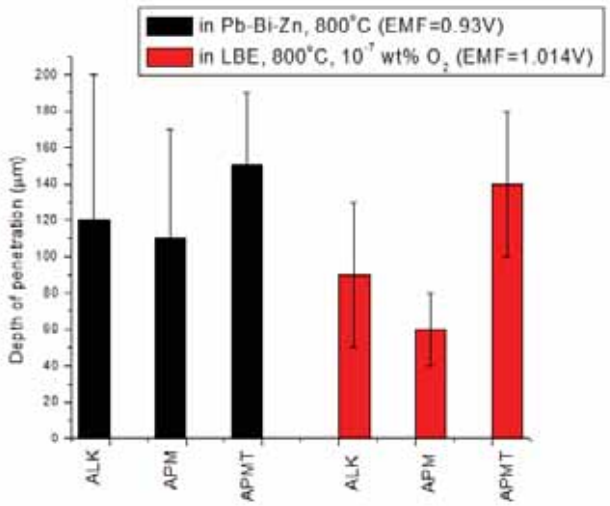

Figure 14. Depth of penetration of liquid Pb-Bi-Zn and LBE into bulk structural materials (Kanthal steels), at 800 °C and low oxygen concentration (~10^{-7} w. t.%)

Table 4. Assessment of the thickness loss in Kanthal samples, Pb-Bi-Zn alloy vs. LBE (800 °C, low oxygen content)

Kanthal sample	*thickness loss (μm)*	
	in Pb-Bi-Zn (800C, 10^{-7} w. t.% O_2)	in LBE (800 C, low O_2 conc.)
ALK	120 ± 80	90 ±40
APM	110 ± 60	60 ±20
APMT	150 ± 40	140 ± 40

6. CONCLUSIONS

Three liquid-metal alloys that are potential candidates for use in solar thermal and nuclear power plant technologies have been tested in static corrosion tests at high temperatures (700-800 °C): lead-bismuth eutectic, Rose's metal and Pb-Bi-Zn eutectic. Three Kanthal steels (ALK, APM and APMT) were investigated as potential structural materials. Tests in which the structural material samples were immersed in the liquid eutectics were performed at 600–800 °C, with sensor-controlled oxygen concentration and for up to 1000 h. The following conclusions can be pointed out:

1) Oxygen control of the liquid metal in a static corrosion test can be made simply by maintaining an EMF value that is below the EMF line for the dissolution of the protective metal oxides.

2) A linear growth rate of the protective aluminum oxide layers on the Kanthal steels has been observed at 700 and 800 °C in LBE (when massive dissolution is not present). Dissolution occurs on APM and APMT in Rose and LBE. Detachment and layer re-growth prevent a precise oxide thickness determination.

3) ALK steel experiences a corrosion rate of less than 150 μm per year at a temperature of 800 °C under static test conditions in LBE and in Rose's metal. Higher corrosion rates are found in APM and APMT.

4) Since Sn is a stronger oxidizer than Pb and Bi, corrosion process in Rose's metal is more aggressive than in LBE. An additional issue here is a more frequent detachment of Al-oxide and lack of its re-growth in Rose's metal. Because of these reasons, this alloy has been abandoned for further research.

5) Pb-Bi-Zn eutectic has at least two serious drawbacks: a strong interaction at the sample-holder interface, and a huge bulk material loss in structural metal (steels) through the formation of non-protective intermetallics.

Results of these tests showed that LBE is by far the most promising candidate so far, in contrast to the investigated liquid Pb-Bi-Sn and Pb-Bi-Zn eutectic systems.

7. ACKNOWLEDGEMENT

This work is based upon the SunShot research project granted by the Department of Energy under Award Number DE-EE0005941.

8. REFERENCES

[1] M. S. El-Genk, J.-M. P. Tournier, *Uses of liquid-metal and water heat pipes in space reactor power systems*, Frontiers in Heat Pipes, Vol. 2 (2011) 013002.

[2] H. Khatib, *IEA World Energy outlook 2010*, *Ener. Pol.,* Vol. 39 (2011) 2507−2511.

[3] J. Hinkley, B. Curtin, *Concentrating Solar Power-Drivers and Opportunities for Cost-Competitive Electricity*, Commonwealth Scientific and Industrial Research Organisation (CSIRO), Australia (2011).

[4] A. M. Bassily, *Modeling, numerical optimization, and irreversibility reduction of a triple-pressure reheat combined cycle*, Energy, Vol. 32 (2007) 778−794.

[5] D. Frazer, E. Stergar, C. Cionea, P. Hosemann, *Liquid metal as a heat transport fluid for thermal solar power applications*, SolarPACES 2013, Energy Procedia, Vol. 49 (2014) 627–636.

[6] R. O. Scarlat, P. F. Peterson, *The current status of fluoride salt cooled high temperature reactor (FHR) technology and its overlap with HIF target chamber concepts*, Nucl. Instr. and Meth. in Phys. Res. A, Vol. 733 (2014) 57−64.

[7] Idaho National Laboratory Lead-Cooled Fast Reactor (LFR) Fact Sheet: http://www4vip.inl.gov/research/lead-cooled-fast-reactor/.

[8] J. Zhang, N. Li, *Review of the studies on fundamental issues in LBE corrosion*, J. Nucl. Mat., Vol. 373 (2008) 351–377.

[9] J. Abella, A. Verdaguer, S. Colominas, K Ginestar, L. Martinelli, *Fundamental data: solubility of nickel and oxygen and diffusivity of iron and oxygen in molten LBE*, J. Nucl. Mat., Vol. 415 (2011) 329−337.

[10] Ellingham Index Page: http://www.engr.sjsu.edu/ellingham/.

[11] Handbook on Lead-bismuth Eutectic Alloy and Lead Properties, Materials Compatibility, Thermal-hydraulics and Technologies, 2007 ed., Nuclear Energy Agency, Organisation for Economic Co-Operation and Development (NEA/OECD), Paris, France, 2007.

[12] B. F. Gromov, Y. I. Orlov, P. N. Martynov, V. A. Gulevsky, *The problems of technology of the heavy liquid metal coolants (lead-bismuth, lead)*, Nucl. Eng. Des., Vol. 173 (1997).

[13] C. Schroer, J. Konys, *Physical Chemistry of Corrosion and Oxygen Control in Liquid Lead and Lead-Bismuth Eutectic* (Wissenschaftliche Berichte, FZKA 7364), Karlsruhe 2007. (https://www.deutsche-digitale-bibliothek.de/binary/UXLSJBDAKUYFBCOB6OENDWQCLUZX4Y24/full/1.pdf).

[14] *High Operating Temperature Heat Transfer Fluids for Solar Thermal Power Generation*, DOE Project Grant (UCLA) DE-EE0005941, Annual report for 2014.

[15] P. Hosemann, M. de Caro, K. Woloshun, F. Rubio, S. A. Maloy, *Heavy Liquid Metal Corrosion of Structural Materials in Advanced Nuclear Systems*, JOM: the journal of the Minerals, Metals & Materials Society 07/2013; 65(8).

[16] P. Hosemann, R. Dickerson, P. Dickerson, N. Li, S. A. Maloy, *Transmission electron microscopy (TEM) on oxide layers formed on D9 stainless steel in lead bismuth eutectic (LBE)*, Corr. Sci., Vol. 66 (2013) 196−202.

[17] A. M. Bolind, A. P. Shivprasad, D. Frazer, P. Hosemann, *Essential aspects of control-ling the oxygen content of molten tin in engineering applications*, Mat. Des., Vol. 52 (2013) 168−178.

ТЕЧНИ Pb-Bi ЕУТЕКТИК КАО МАТЕРИЈАЛ ЗА ПРЕНОС ТОПЛОТЕ У НУКЛЕАРНИМ РЕАКТОРИМА ЧЕТВРТЕ ГЕНЕРАЦИЈЕ, И ВИСОКОТЕМПЕРАТУРНИМ КОНЦЕНТРАТОРИМА СОЛАРНЕ ЕНЕРГИЈЕ: КАРАКТЕРИСТИКЕ, ЗАХТЕВИ, ПОТЕШКОЋЕ

Сажетак: Течни тешки метали нашли су широк спектар примена у системима за конверзију енергије, због њихових добрих термалних својстава, а особито због ниске тачке топљења и могућности рада на вишим температурама без кључања. Штавише, неутронска својства различитих течних метала чине их погодним за фузионе реакторе, као и за нуклеарне реакторе IV генерације. У најновије време, системи за концентровање соларне енергије се све више усмеравају ка овој технологији, пошто омогућава радне температуре и до 800 °C. Главни изазов у њеном практичном реализовању је наћи одговарајуће структурне материјале који би били отпорни на корозију и обезбеђивали механичку снагу током рада. Олово-бизмут еутектик (LBE) је један од главних кандидата за ове примене (у реакторима хлађеним течним металима, и соларним системима) због својих физичких особина: добре топлотне проводљивости, малог топлотног ширења, ниске тачке топљења, неагресивне реактивности према води и малог апсорбовања неутрона. Главни ограничавајући фактор за његову употребу је изразита корозивност према челику и другим структурним материјалима. Овде доносимо резултате систематског испитивања материјала у течном Pb-Bi еутектику (LBE) и његовим алтернативама. Различити потенцијални структурни материјали су тестирани у LBE-у, Роузовом металу (Bi-Pb-Sn) и у Pb-Bi-Zn еутектику, у статичким условима корозије. Посткорозиона карактеризација рађена је микроструктурном анализом (SEM/EDS, дифракција x-зрачења, Раманова спектроскопија), уз евалуацију могућих механизама корозије.

Кључне ријечи: течни метали, олово-бизмут еутектик, соларна енергија, нуклеарна постројења, корозија, челик.